Journal of Engineering Science and Technology
Vol. 18, No. 4 (2023) 2148 - 2160
© School of Engineering, Taylor's University

# PREDICTIVE MODELING OF DIMENSIONAL ACCURACIES IN 3D PRINTING USING ARTIFICIAL NEURAL NETWORK

SIVARAO S.[1,*], K. KUMARAN[2], DHARSYANTH[1], M. AMRAN[1], S. M. SHUKOR[1], S. PUJARI[3], D. RAMASAMY[4], U. K. VATESH[5], ABDULKAREEM SH. MAHDI AL-OBAIDI[6], S. RAMESH[7,8], K. Y. SARA LEE[9]

[1] Faculty of Manufacturing Engineering, Universiti Teknikal Malaysia Melaka, 76100 Durian Tunggal, Melaka, Malaysia
[2] Faculty of Mechanical and Automotive Engineering Technology, Universiti Malaysia Pahang, 26600 Pekan, Pahang, Malaysia
[3] Lendi Institute of Engineering and Technology, Vizianagaram, 535005, Andhra Pradesh, India
[4] Department of Mechanical Engineering, College of Engineering, Universiti Malaysia Pahang, 26300 Gambang, Pahang, Malaysia
[5] Mechanical Engineering Department, Amity University, 201301, Uttar Pradesh, Noida, India
[6] School of Engineering, Faculty of Innovation and Technology, Taylor's University, Taylor's Lakeside Campus, Subang Jaya, Selangor DE, Malaysia
[7] Center of Advanced Manufacturing and Material Processing, Department of Mechanical Engineering, Faculty of Engineering, University of Malaya, 50603 Kuala Lumpur, Malaysia
[8] Universiti Tenaga Nasional, Putrajaya Campus, Jalan IKRAM-UNITEN, 43000 Kajang, Selangor, Malaysia
[9] Center of Systematic Innovation Research, Department of Mechanical Engineering, Faculty of Engineering and Technology, Tunku Abdul Rahman University of Management and Technology, 53300 Kuala Lumpur, Malaysia
* Corresponding Author: sivarao@utem.edu.my

## Abstract

Additive manufacturing, particularly Fused Deposition Modeling (FDM) using three-dimensional (3D) printing, has revolutionized the manufacturing industry by offering design flexibility, customization options, affordability, and high printing speed. However, improper selection of process parameters in FDM can lead to suboptimal surface efficiency, defective mechanical properties, increased waste, and higher production costs. In this research, an Artificial Neural Network (ANN) model was developed to optimize dimensional properties in FDM by considering control factors such as layer thickness, orientation, raster angle, raster width, and air gap. Experimental data consisting of 27 sets of control parameters and corresponding dimensional outputs were used to train and validate the ANN model. The ANN model was developed using MATLAB software, employing training functions and learning algorithms to optimize the neural network architecture. The optimized ANN structure comprised 15 neurons and 2 layers, and it demonstrated accurate prediction of dimensional properties with percentage errors ranging from 0.01% to 25.49% for length, less than 10% for weight, and less than 4% for thickness. The mean absolute percentage error (MAPE) and root mean square error (RMSE) were used to quantify the errors, indicating the effectiveness of the ANN model in predicting dimensional properties. The results highlight the potential of ANN in optimizing FDM process parameters for improved dimensional accuracy. The ANN model provides a reliable tool for manufacturers to predict and optimize the length, weight, and thickness of 3D-printed components, leading to enhanced product quality and reduced production costs. The developed ANN model can be further extended to consider other parameters and optimize various aspects of the additive manufacturing process.

Keywords: Additive manufacturing, Artificial neutral network, Dimensional accuracy, Fused deposition modelling, Predictive modelling.

## 1. Introduction

The introduction of additive manufacturing has been a game-changer in the manufacturing industry, providing numerous advantages over traditional processes such as Computer Numerical Control (CNC) machining. One of the key benefits of three-dimensional (3D) printing, particularly the Fused Deposition Modelling (FDM) technique, is its ability to empower manufacturers with design flexibility and customization options. Unlike conventional methods, 3D printing allows for on-demand modifications without disrupting the production line. Additionally, FDM stands out among the various additive manufacturing techniques due to its affordability and high printing speed, making it a popular choice for manufacturers seeking efficient and cost-effective manufacturing solutions [1-3].

In particular, 3D melting and solidification-based printing offers several advantages, including high accuracy, nanometre resolution, minimal material waste, minimal roughness, and ease of assembly [4]. However, the improper selection of process or control parameters can lead to low surface efficiency, defective mechanical properties, increased waste and processing time, resulting in higher production costs and resource consumption [5]. The critical control factors for FDM methods are the raster angle, raster width, air gap, layer thickness, and component orientation [6, 7]. The layer thickness refers to the height of the materials accumulated along the Z-axis, which is typically the vertical axis of the FDM unit. It is usually smaller than the extruder nozzle diameter and depends on the nozzle diameter. Project orientation is characterized by the orientation of the part along the X-axis, Y-axis, and Z-axis on the build platform. The raster angle represents the direction of the deposition bead with respect to the X-axis of the build platform in the FDM machine. Raster width is defined as the width of the deposition beads and depends on the extrusion nozzle diameter. The air gap refers to the gap between two adjacent rasters on a deposited layer. The air gap is considered negative when two adjacent layers overlap [8].

Various parameters are crucial for evaluating the quality of 3D printing components produced through additive manufacturing processes. These parameters encompass dimensional accuracy, mechanical strength, surface roughness, design duration, post-processing requirements, and material properties. In the existing literature, many studies have primarily focused on mechanical performance, tribological properties, rheological properties, and other related factors [6, 7, 9, 10]. While certain parameters are widely recognized as quality indicators, such as dimensional accuracy and mechanical strength, the inclusion of parameters such as length, weight, and thickness may require further investigation and clarification. Although not traditionally exclusively associated with quality, these parameters significantly influence the outcome of the printing process. Attaining precise dimensions, appropriate weight, and the desired thickness is essential for ensuring the functionality and performance of the printed components in diverse applications [11, 12].

Machine learning is gaining momentum and playing a crucial role in enhancing various aspects of 3D printing processes. Its applications span across process optimization, dimensional accuracy analysis, manufacturing defect detection, and material property prediction [13, 14]. Artificial Neural Networks (ANN) are highly interconnected networks of basic components called neurons, which can perform linear or non-linear scalar transformations and are connected by weighted connections. With input from measured data, neural networks are well-suited for tasks such as classification, estimation, simulation, and prediction of desired properties [15-17]. In the context of control parameters and responses, ANNs can be trained to learn and represent the complex relationship between these variables. To use ANN for presenting the relationship, a dataset containing inputs (control parameters) and corresponding outputs (responses) is required. The ANN is then trained using this dataset, adjusting the connection weights between neurons to minimize the difference between the predicted outputs and the actual outputs. Once the ANN is trained, it can be used to predict the responses for new sets of control parameters that were not present in the training dataset. By feeding the control parameter values into the trained ANN, it can generate predicted responses, providing insights into how changes in the control parameters affect the outcomes. In one study, an ANN model was developed to predict surface roughness based on two process parameters: deposition angle and layer thickness [18]. Similarly, in another study, an ANN model was optimized for various process parameters, including layer thickness, build orientation, infill density, and number of contours, to enhance the dimensional precision (length, width, and thickness) of FDM printed parts [19]. In another study, different decision tree algorithms were employed to predict surface roughness in polyethylene terephthalate glycol (PETG) parts printed using the FDM technique. The relevant attributes considered were layer height, extrusion temperature, print speed, print acceleration, and flow rate [20].

In summary, ANN has the potential to predict dimensional properties such as length, width, and thickness based on control factors or process parameters. The research conducted holds significant practical implications for the field of additive manufacturing. The research in this paper has practical implications for additive manufacturing. The findings provide insights for optimizing manufacturing processes, enabling customized part design, accelerating prototyping, improving quality control, exploring material-specific behaviours, and integrating with automation. These practical implications open up new opportunities for efficient production, personalized manufacturing, rapid innovation, and enhanced automation in additive manufacturing. The goal of the current work is to develop a predictive ANN model that can optimize the dimensional properties by considering control factors such as layer thickness, orientation, air gap, raster angle, and width.

## 2. Methodology

### 2.1. Control Factors

The control factors and their respective levels for predicting the quality of 3D printing are presented in Table 1. Traditionally, when employing a conventional structure with five control factors at three levels, it would necessitate conducting 243($3^5$) experiments. However, by utilizing the Taguchi approach, it becomes possible to achieve similar results with fewer studies. In this research, a feed-forward neural network (NN) incorporating the backpropagation (BP) algorithm was employed to construct multiple models for optimizing input and output. The control factors employed for prediction using the ANN included layer thickness, orientation, raster angle, raster width, and air gap. These control factors served as inputs for the ANN architecture, while the desired outputs for prediction were the length, width, and thickness. A total of 27 sets of experiments were adopted according to the control factors as presented in Table 2 [21]. The development of this multi-input and output ANN feature aims to create an adaptive system capable of continuous monitoring of various parameters.

**Table 1. Control factors and the respective levels [21].**

| Control Factors | Symbol | Levels 1 | Levels 2 | Levels 3 |
|---|---|---|---|---|
| **Layer thickness/mm** | A | 0.127 | 0.178 | 0.254 |
| **Orientation/°** | B | 0 | 15 | 30 |
| **Raster angle/°** | C | 0 | 30 | 60 |
| **Raster width/mm** | D | 0.406 | 0.456 | 0.506 |
| **Air gap/mm** | E | 0 | 0.004 | 0.008 |

**Table 2. Experiment data [21].**

| | Input | | | | | Output | | |
|---|---|---|---|---|---|---|---|---|
| **Exp. No.** | **Layer thickness/mm** | **Orientation/°** | **Raster angle/°** | **Raster width/ mm** | **Air gap/mm** | ***ΔL*** | ***ΔW*** | ***ΔT*** |
| **1** | 0.127 | 0 | 0 | 0.406 | 0 | 0.0461 | 0.0598 | 0.1167 |
| **2** | 0.127 | 15 | 0 | 0.456 | 0.004 | 0.0958 | 0.0434 | 0.1565 |
| **3** | 0.127 | 30 | 0 | 0.503 | 0.008 | 0.0852 | 0.0832 | 0.1034 |
| **4** | 0.127 | 0 | 30 | 0.456 | 0.004 | 0.0387 | 0.0732 | 0.1065 |
| **5** | 0.127 | 15 | 30 | 0.506 | 0.008 | 0.1528 | 0.0498 | 0.1532 |
| **6** | 0.127 | 30 | 30 | 0.406 | 0 | 0.1414 | 0.0434 | 0.1067 |
| **7** | 0.127 | 0 | 60 | 0.506 | 0.008 | 0.0227 | 0.0534 | 0.1265 |
| **8** | 0.127 | 15 | 60 | 0.406 | 0 | 0.1101 | 0.0665 | 0.1601 |
| **9** | 0.127 | 30 | 60 | 0.456 | 0.004 | 0.0941 | 0.0634 | 0.1498 |
| **10** | 0.178 | 0 | 0 | 0.456 | 0.008 | 0.098 | 0.201 | 0.1067 |
| **11** | 0.178 | 15 | 0 | 0.506 | 0 | 0.0265 | 0.0765 | 0.1732 |
| **12** | 0.178 | 30 | 0 | 0.406 | 0.004 | 0.0561 | 0.0498 | 0.1801 |
| **13** | 0.178 | 0 | 30 | 0.506 | 0 | 0.0772 | 0.0367 | 0.1466 |
| **14** | 0.178 | 15 | 30 | 0.406 | 0.004 | 0.1127 | 0.0434 | 0.1932 |
| **15** | 0.178 | 30 | 30 | 0.456 | 0.008 | 0.1058 | 0.0366 | 0.1801 |
| **16** | 0.178 | 0 | 60 | 0.406 | 0.004 | 0.0607 | 0.0367 | 0.1198 |
| **17** | 0.178 | 15 | 60 | 0.456 | 0.008 | 0.0732 | 0.0665 | 0.1701 |
| **18** | 0.178 | 30 | 60 | 0.506 | 0 | 0.0381 | 0.0365 | 0.1465 |
| **19** | 0.254 | 0 | 0 | 0.506 | 0.004 | 0.543 | 0.0198 | 0.2634 |
| **20** | 0.254 | 15 | 0 | 0.406 | 0.008 | 0.507 | 0.0421 | 0.3832 |

| | | | | | | | | |
|---|---|---|---|---|---|---|---|---|
| **21** | 0.254 | 30 | 0 | 0.456 | 0 | 0.119 | 0.0238 | 0.3768 |
| **22** | 0.254 | 0 | 30 | 0.406 | 0.008 | 0.0332 | 0.0182 | 0.3464 |
| **23** | 0.254 | 15 | 30 | 0.456 | 0 | 0.0285 | 0.0401 | 0.4199 |
| **24** | 0.254 | 30 | 30 | 0.506 | 0.004 | 0.0972 | 0.0299 | 0.0232 |
| **25** | 0.254 | 0 | 60 | 0.456 | 0 | 0.0199 | 0.0281 | 0.2635 |
| **26** | 0.254 | 15 | 60 | 0.506 | 0.004 | 0.0485 | 0.0401 | 0.3432 |
| **27** | 0.254 | 30 | 60 | 0.008 | 0.008 | 0.0207 | 0.04 | 0.3065 |

## 2.2. Developing the ANN utilizing experimental data

As in the flow chart in Fig. 1, the ANN methodology involved gathering data for tasks such as network creation, network configuration, weight and bias initialization, network training, network validation, and data analysis. Artificial neural network structures, which encompass comprehensive computational algorithms for knowledge exploration, offer significant potential for leveraging the information available in computer libraries.

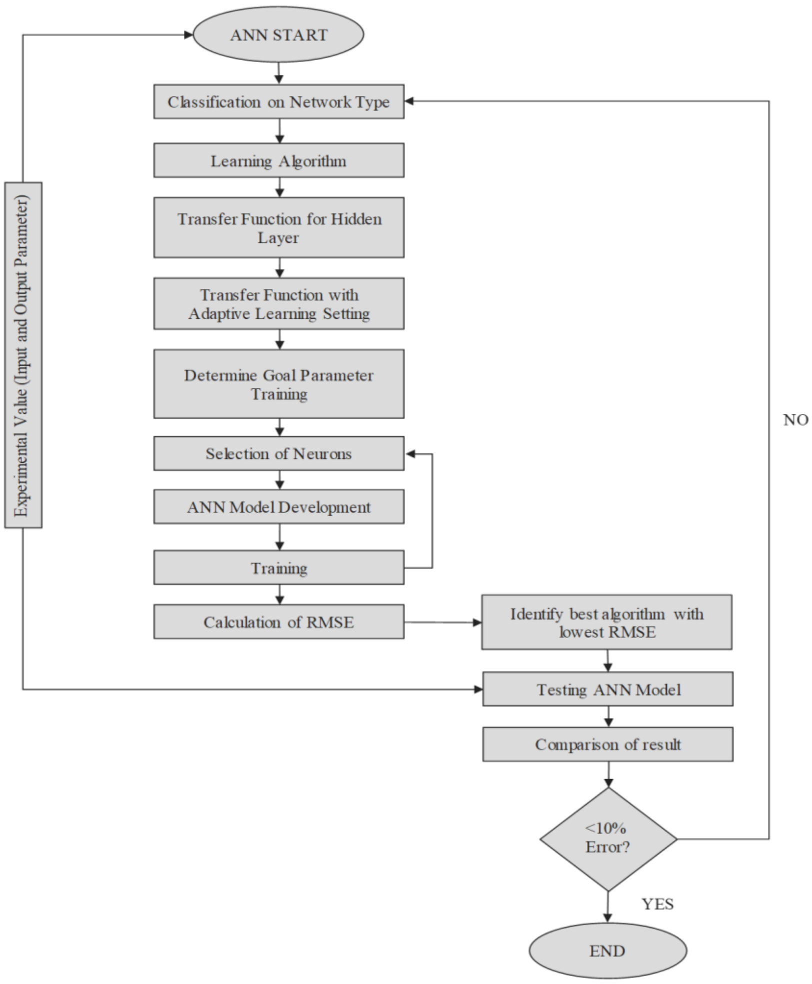


**Fig. 1. Flowchart of developing ANN.**

The training of the ANN was performed using MATLAB r2019b software. The input data (layer thickness, orientation, raster angle, raster width, and air gap) and output data (length, width, and thickness) were collected and imported into the MATLAB software. Afterwards, the ANN structure was created with a defined number of neurons and layers, as depicted in Fig. 2.

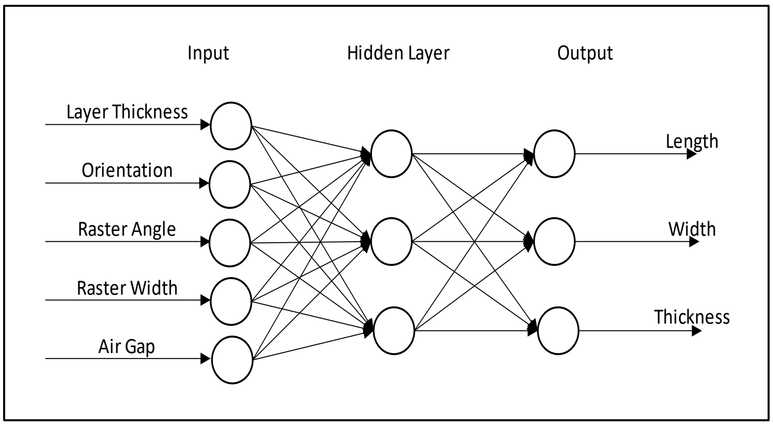


**Fig. 2. The schematic ANN structure of this research for quality.**

In developing the ANN framework in MATLAB, two datasets were categorized into a ratio of 70% and 30%. The training dataset, which comprised 70% (18) of the data, was used to train the ANN system, while the remaining 30% (9) was reserved for validation purposes. The training data was selected randomly from the original 27 experimental data points, resulting in a total of 18 data points. This process involved passing the data through the network, estimating errors, and optimizing the neural connections to minimize these errors. Finally, the trained output data underwent testing, representing the final step in the development of the ANN using MATLAB software.

The performance of the neural network was assessed by subjecting it to experimental data testing. Evaluating the errors played a vital role in determining the effectiveness of the ANN. In this regard, error equations including the Mean Absolute Percentage Error (MAPE) and Root Mean Square Error (RMSE), were utilized to calculate and quantify the errors. Following the completion of the training process, the model underwent testing using additional experimental data to further validate its performance.

## 3. Results and Discussion

### 3.1. ANN Optimization for Quality

The MATLAB Neural Network Toolbox offers a wide range of training and learning capabilities. In this study, the training functions employed were TRAINLM and TRAINSG. Additionally, LEARNGDM was utilized to adapt the network to the Gradient Descent Momentum weight and bias learning feature, which had an impact on the Mean Square Error (MSE). For this research, an optimized parameter setting for the ANN architecture was used, consisting of 15 neurons and 2 layers. The number of neurons depended on the number of input parameters utilized. Throughout the analysis, various ANN configurations were evaluated by varying the number of neurons in the hidden layer. Iterative processes and different transfer functions were tested to determine the most effective approach for predicting the consistency parameters. The ANN training and architectural parameters can be found in Table 3. Ultimately, Network 3 was selected as the best network due to its low percentage error value of 3.951%. The optimized neural network tool is presented in Fig. 3.

**Table 3. ANN training and architectural parameters.**

| No. of Run | 1 | 2 | 3 |
|---|---|---|---|
| **Network Name** | Network1 | Network2 | Network3 |
| **Network Type** | FeedForward | FeedForward | FeedForward |
| **Training Func** | TRAINLM | TRAINLM | TRAINLM |
| **Adaptive Learning Func** | LEARNGDM | LEARNGDM | LEARNGDM |
| **No of Neurons** | 10 | 12 | 15 |
| **Transfer Func** | TANSIG | TANSIG | TANSIG |
| **goal** | 0 | 1.00E-04 | 1.00E-05 |
| **min_grad** | 1.00E-05 | 1.00E-04 | 1.00E-06 |
| **mu** | 1.00E-05 | 1.00E-04 | 1.00E-05 |

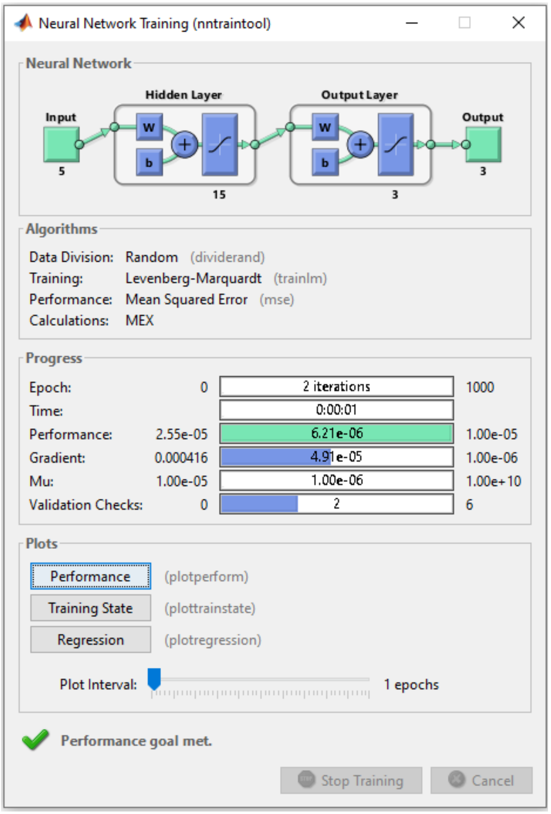


**Fig. 3. Optimized neural network training tool.**

Table 4, 5, and 6 present a comparison between the experimental and ANN predicted results for the training data, specifically for length, weight, and thickness, respectively. In terms of length prediction, the percentage error between the experimental and predicted values ranged from 0.01% to 25.49%. It was found that 83% of the datasets had a percentage error of less than 6% for length prediction. For weight prediction, 72% of the datasets had a percentage error of less than 10%, with the highest percentage error being 53.12%. Furthermore, the current model demonstrated effective prediction of thickness, with all datasets achieving a percentage error of less than 4%.

**Table 4. Comparison between experimental and ANN predicted result of training data for length.**

| No | Input Data | | | | | Output Length Δ*L* | | |
|---|---|---|---|---|---|---|---|---|
| | Layer thickness/mm | Orientation/° | Raster angle/° | Raster width/mm | Air gap/mm | Experimental | Predicted | Percentage Error (%) |
| **1** | 0.127 | 0 | 0 | 0.406 | 0 | 0.0461 | 0.0461 | 0.09 |
| **2** | 0.127 | 15 | 0 | 0.456 | 0.004 | 0.0958 | 0.0958 | 0.01 |
| **3** | 0.127 | 30 | 0 | 0.506 | 0.008 | 0.0852 | 0.0852 | 0.04 |
| **4** | 0.127 | 0 | 30 | 0.456 | 0.004 | 0.0387 | 0.0383 | 1.02 |
| **5** | 0.127 | 15 | 30 | 0.506 | 0.008 | 0.1528 | 0.1494 | 2.21 |
| **6** | 0.127 | 30 | 30 | 0.406 | 0 | 0.1414 | 0.1409 | 0.32 |
| **7** | 0.178 | 15 | 0 | 0.506 | 0 | 0.0265 | 0.0292 | 10.32 |
| **8** | 0.178 | 30 | 0 | 0.406 | 0.004 | 0.0561 | 0.0559 | 0.33 |
| **9** | 0.178 | 0 | 30 | 0.506 | 0 | 0.0772 | 0.0777 | 0.62 |
| **10** | 0.178 | 15 | 30 | 0.406 | 0.004 | 0.1127 | 0.1125 | 0.14 |
| **11** | 0.178 | 30 | 30 | 0.456 | 0.008 | 0.1058 | 0.1055 | 0.27 |
| **12** | 0.178 | 0 | 60 | 0.406 | 0.004 | 0.0607 | 0.0606 | 0.18 |
| **13** | 0.254 | 30 | 0 | 0.456 | 0 | 0.119 | 0.1181 | 0.72 |
| **14** | 0.254 | 0 | 30 | 0.406 | 0.008 | 0.0332 | 0.0352 | 6.11 |
| **15** | 0.254 | 15 | 30 | 0.456 | 0 | 0.0285 | 0.0278 | 2.29 |
| **16** | 0.254 | 30 | 30 | 0.506 | 0.004 | 0.0972 | 0.0971 | 0.14 |
| **17** | 0.254 | 0 | 60 | 0.456 | 0 | 0.0199 | 0.0251 | 25.49 |
| **18** | 0.254 | 15 | 60 | 0.506 | 0.008 | 0.0485 | 0.0418 | 13.74 |

**Table 5. Comparison between experimental and ANN predicted result of training data for weight.**

| No. | Input Data | | | | | Output Weight *ΔW* | | |
|---|---|---|---|---|---|---|---|---|
| | Layer thickness/mm | Orientation/° | Raster angle/° | Raster width/mm | Air gap/mm | *Experimental* | *Predicted* | *Percentage Error (%)* |
| **1** | 0.127 | 0 | 0 | 0.406 | 0 | 0.0598 | 0.0586 | 2.08 |
| **2** | 0.127 | 15 | 0 | 0.456 | 0.004 | 0.0434 | 0.0448 | 3.17 |
| **3** | 0.127 | 30 | 0 | 0.506 | 0.008 | 0.0832 | 0.0798 | 4.10 |
| **4** | 0.127 | 0 | 30 | 0.456 | 0.004 | 0.0732 | 0.0728 | 0.53 |
| **5** | 0.127 | 15 | 30 | 0.506 | 0.008 | 0.0498 | 0.0493 | 1.00 |
| **6** | 0.127 | 30 | 30 | 0.406 | 0 | 0.0434 | 0.0436 | 0.46 |
| **7** | 0.178 | 15 | 0 | 0.506 | 0 | 0.0762 | 0.0764 | 0.27 |
| **8** | 0.178 | 30 | 0 | 0.406 | 0.004 | 0.0498 | 0.0499 | 0.11 |

| | | | | | | | | |
|---|---|---|---|---|---|---|---|---|
| **9** | 0.178 | 0 | 30 | 0.506 | 0 | 0.0367 | 0.0377 | 2.76 |
| **10** | 0.178 | 15 | 30 | 0.406 | 0.004 | 0.0434 | 0.0336 | 22.52 |
| **11** | 0.178 | 30 | 30 | 0.456 | 0.008 | 0.0366 | 0.0369 | 0.95 |
| **12** | 0.178 | 0 | 60 | 0.406 | 0.004 | 0.0367 | 0.0366 | 0.37 |
| **13** | 0.254 | 30 | 0 | 0.456 | 0 | 0.0238 | 0.0271 | 13.69 |
| **14** | 0.254 | 0 | 30 | 0.406 | 0.008 | 0.0182 | 0.0209 | 14.64 |
| **15** | 0.254 | 15 | 30 | 0.456 | 0 | 0.0401 | 0.0393 | 1.98 |
| **16** | 0.254 | 30 | 30 | 0.506 | 0.004 | 0.0299 | 0.0304 | 1.64 |
| **17** | 0.254 | 0 | 60 | 0.456 | 0 | 0.0281 | 0.0251 | 10.62 |
| **18** | 0.254 | 15 | 60 | 0.506 | 0.008 | 0.0401 | 0.0188 | 53.12 |

**Table 6. Comparison between experimental and ANN predicted result of training data for thickness.**

| **No.** | **Input Data** | | | | | **Output Thickness $\Delta T$** | | |
|---|---|---|---|---|---|---|---|---|
| | **Layer thickness/mm** | **Orientation/°** | **Raster angle/°** | **Raster width/mm** | **Air gap/mm** | ***Experimental*** | ***Predicted*** | ***Percentage Error (%)*** |
| **1** | 0.127 | 0 | 0 | 0.406 | 0 | 0.1167 | 0.1174 | 0.58 |
| **2** | 0.127 | 15 | 0 | 0.456 | 0.004 | 0.1565 | 0.1565 | 0.01 |
| **3** | 0.127 | 30 | 0 | 0.506 | 0.008 | 0.1034 | 0.1044 | 1.01 |
| **4** | 0.127 | 0 | 30 | 0.456 | 0.004 | 0.1065 | 0.1066 | 0.08 |
| **5** | 0.127 | 15 | 30 | 0.506 | 0.008 | 0.1532 | 0.1533 | 0.07 |
| **6** | 0.127 | 30 | 30 | 0.406 | 0 | 0.1067 | 0.1061 | 0.58 |
| **7** | 0.178 | 15 | 0 | 0.506 | 0 | 0.1732 | 0.1778 | 2.64 |
| **8** | 0.178 | 30 | 0 | 0.406 | 0.004 | 0.1801 | 0.1805 | 0.23 |
| **9** | 0.178 | 0 | 30 | 0.506 | 0 | 0.1466 | 0.1465 | 0.06 |
| **10** | 0.178 | 15 | 30 | 0.406 | 0.004 | 0.1932 | 0.1857 | 3.91 |
| **11** | 0.178 | 30 | 30 | 0.456 | 0.008 | 0.1801 | 0.1808 | 0.40 |
| **12** | 0.178 | 0 | 60 | 0.406 | 0.004 | 0.1198 | 0.1199 | 0.11 |
| **13** | 0.254 | 30 | 0 | 0.456 | 0 | 0.3768 | 0.3789 | 0.55 |
| **14** | 0.254 | 0 | 30 | 0.406 | 0.008 | 0.3464 | 0.3459 | 0.15 |
| **15** | 0.254 | 15 | 30 | 0.456 | 0 | 0.4199 | 0.4176 | 0.54 |
| **16** | 0.254 | 30 | 30 | 0.506 | 0.004 | 0.2565 | 0.2566 | 0.04 |
| **17** | 0.254 | 0 | 60 | 0.456 | 0 | 0.2635 | 0.2619 | 0.62 |
| **18** | 0.254 | 15 | 60 | 0.506 | 0.008 | 0.3432 | 0.3561 | 3.76 |

## 3.2. ANN Prediction for Quality

The neural network model was developed using a feed-forward backpropagation architecture with 5-15-3 neurons, as illustrated in Fig. 3. Out of the 27 experimental data points, 18 were selected for training the ANN in this model, while the remaining data points were used for evaluation. The selection of training and evaluation data was performed randomly.

Based on Fig. 4, the training of the model was stopped when the validation error increased at epoch 2. The figure indicates that the best validation performance at epoch 0 was 1.3398e-06. Furthermore, referring to Fig. 5, the regression plots for training, validation, testing, and overall were found to be 0.99845, 0.99996, 0.99996, and 0.99907, respectively. These values indicate a strong linear relationship between the model's outputs and the desired goals, as they are close to unity. The output of the ANN model aligns perfectly with the target, and the measured and expected values exhibit remarkable similarity.

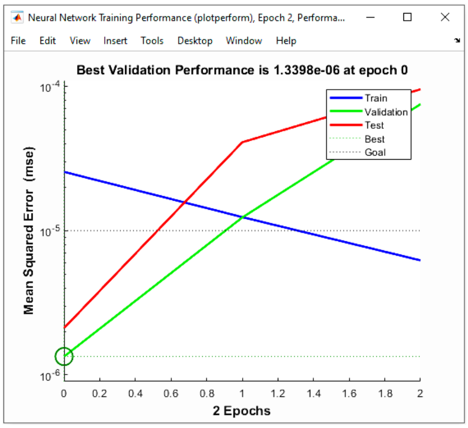


**Fig. 4. Performance plot of dimensional accuracy.**

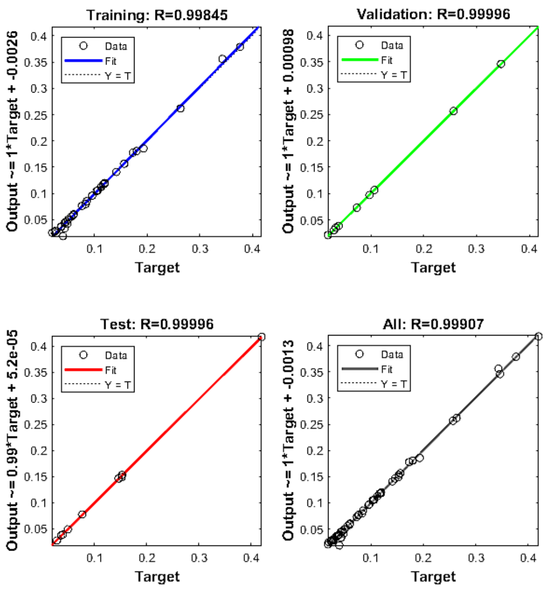


**Fig. 5. Regression plot of dimensional accuracy.**

## 3.3. Model Validation for Quality

The results obtained from the ANN were compared with the experimental data. To evaluate the predictive performance of the models, Root Mean Square Error (RMSE) and Mean Absolute Percentage Error (MAPE) were calculated by comparing the targets and outputs of the ANN model. After successfully completing the training process, the network was tested using additional experimental data. The ANN model's output was calculated by taking into account various parameters.

RMSE is a commonly used metric for measuring the accuracy of a predictive model. It quantifies the average difference between the predicted values of a model and the actual values in a dataset. The RMSE value was calculated using Equation

(1) and computed in MATLAB. Tables 7 and 8 present the RMSE values between the actual and predicted values for the training and validation datasets, respectively. The optimized number of neurons, determined by selecting the one with the lowest RMSE value, is 15. For the training dataset, the RMSE values for length, width, and thickness are all below 0.0057. The validation datasets further confirm the validity of the optimized model, as all the RMSE values are below 0.0014.

$$RMSE = \sqrt{\frac{\sum_{i=1}^{N}(Predicted_i - Actual_i)^2}{N}} \tag{1}$$

where $Predicted_i$ is the predicted value for the *i*th observation and $Actual_i$ is the observed (actual) value for the *i*th observation, ad N is the total number of observations.

**Table 7. Comparison of RSME value between actual and predicted value for training dataset.**

| No. of Neurons | RMSE for Length | RMSE for Width | RMSE for Thickness |
|---|---|---|---|
| 10 | 0.0034 | 0.0078 | 0.0116 |
| 12 | 0.0231 | 0.0119 | 0.0261 |
| 15 | 0.0023 | 0.0057 | 0.0038 |

**Table 8. Comparison of RSME value between actual and predicted value for validation dataset.**

| No. of Neurons | RMSE for Length | RMSE for Width | RMSE for Thickness |
|---|---|---|---|
| 15 | 0.0011 | 0.0010 | 0.0014 |

On the other hand, MAPE serves as a metric to assess the accuracy of a predictive model by quantifying the percentage deviation from the actual values. It offers a relative measure of the magnitude of errors introduced by the model. The MAPE values were computed using the equation (2). Table 9 presents the MAPE values for the training and validation datasets, including length, width, and thickness parameters. Notably, the MAPE for the training data is below 7.5%, while the MAPE for the validation data is below 3.1%.

$$MAPE = \frac{1}{N}\sum_{i=1}^{n}\left|\frac{Actual_i - Predicted_i}{Actual_i}\right| \times 100 \tag{2}$$

**Table 9. MAPE values for training and validation datasets.**

| Parameter | Training Dataset MAPE (%) | Validation Dataset MAPE (%) |
|---|---|---|
| All | 3.951 | 1.766 |
| Length | 3.557 | 3.066 |
| Width | 7.445 | 1.687 |
| Thickness | 0.851 | 0.546 |

## 4. Conclusions

In this study, an Artificial Neural Network (ANN) model was developed to optimize the dimensional properties of 3D-printed components in the Fused Deposition Modeling (FDM) process. The ANN model demonstrated high accuracy in predicting the length, weight, and thickness of the printed parts, with percentage errors within acceptable limits. The key findings of this study highlight the effectiveness of the ANN model in optimizing FDM process parameters. By considering factors such as layer thickness, orientation, raster angle, raster width, and air gap, the ANN model successfully predicted the dimensional properties of the printed parts. This demonstrates the potential of ANN as a reliable tool for manufacturers to achieve improved dimensional accuracy and enhance the overall quality of 3D-printed components. While the developed ANN model showed promising results in predicting the dimensional properties of 3D-printed components, future work could focus on expanding the model's capabilities. This could include incorporating additional input variables and process parameters to improve accuracy and reliability. Exploring other machine learning algorithms or hybrid models could also be beneficial in enhancing the prediction capabilities.

**Abbreviations**

| | |
|---|---|
| AM | Additive manufacturing |
| ANN | Artificial Neural Network |
| FDM | Fused Deposition Modeling |
| MAPE | Mean Absolute Percentage Error |
| RMSE | Root Mean Square Error |

## References

1. Akbaş, O.E.; Hıra, O.; Hervan, S.Z.; Samankan, S.; and Altınkaynak, A. (2019). Dimensional accuracy of FDM-printed polymer parts. *Rapid Prototyping Journal*, 26(2), 288-298.
2. Hasan, H.; Ahmed, S.; Voldman, R.; and Mehany, M. (2018). Parametric effect on surface finish of three-dimensional printed object. *International Journal of Engineering Materials and Manufacture*, 3(2), 98-104.
3. Lim, I.Y.; Ting, C.H.; Ng, C.K.; Tey, J.Y.; Yeo, W.H.; Singh, R.; Lee, K.Y.S.; Chuah, Y.D.; and Teng, W.D. (2023). 3D printing of high solid loading zirconia feedstock via screw-based material extrusion. *Ceramics International*, 49(15), 24852-24860.
4. Yuan, C.; Wang, F.; Qi, B.; Ding, Z.; Rosen, D.W.; and Ge, Q. (2020). 3D printing of multi-material composites with tunable shape memory behavior. *Materials & Design*, 193, 108785.
5. Saad, M.S.; Mohd, N.A.; Baharudin, M.E.; Zakaria, M.Z.; and Fozi, A. (2019). Optimization of surface roughness in FDM 3D printer using response surface methodology, particle swarm optimization, and symbiotic organism search algorithms. *The International Journal of Advanced Manufacturing Technology*, 105(12), 5121-5137.
6. Amirruddin, M.S.; Ismail, K.I.; and Yap, T.C. (2022). Effect of layer thickness and raster angle on the tribological behavior of 3D printed materials. *Materials Today: Proceedings*, 48(6), 1821-1825.
7. Nabavi-Kivi, A.; Ayatollahi, M.R.; and Razavi, N. (2023). Investigating the effect of raster orientation on fracture behavior of 3D-printed ABS specimens under tension-tear loading. *European Journal of Mechanics - A/Solids*, 99, 104944.

8. Dey, A.; and Yodo, N. (2019). A systematic survey of FDM process parameter optimization and their influence on part characteristics. *Journal of Manufacturing and Materials Processing*, 3(3), 64.
9. Hanon, M.M.; Dobos, J.; and Zsidai, L. (2021). The influence of 3D printing process parameters on the mechanical performance of PLA polymer and its correlation with hardness. *Procedia Manufacturing*, 54, 244-249.
10. Naik, M.; Thakur, D.G.; and Chandel, S. (2022). An insight into the effect of printing orientation on tensile strength of multi-infill pattern 3D printed specimen: experimental study. *Materials Today: Proceedings*, 62, 7391-7395.
11. Marrey, M.; Malekipour, E.; El-Mounayri, H.; and Faierson, E.J. (2019). A framework for optimizing process parameters in powder bed fusion (PBF) process using artificial neural network (ANN). *Procedia Manufacturing*, 34, 505-515.
12. Vidakis, N.; David, C.; Petousis, M.; Sagris, D.; Mountakis, N.; and Moutsopoulou, A. (2022). The effect of six key process control parameters on the surface roughness, dimensional accuracy, and porosity in material extrusion 3D printing of polylactic acid: prediction models and optimization supported by robust design analysis. *Advances in Industrial and Manufacturing Engineering*, 5, 100104.
13. Yu, C.; and Jiang, J. (2020). A perspective on using machine learning in 3D bioprinting. *International Journal of Bioprinting*, 6(1), 253.
14. Geng, S.; Luo, Q.; Liu, K.; Li, Y.; Hou, Y.; and Long, W. (2023). Research status and prospect of machine learning in construction 3D printing. *Case Studies in Construction Materials*, 18, e01952.
15. Yee, S.L.K.; and Raymond, W.J.K. (2020). Pneumonia diagnosis using chest X-ray images and machine learning. *Proceedings of the 2020 10th International Conference on Biomedical Engineering and Technology*. Tokyo, Japan, 101-105.
16. Kumar, M.N.; Rastogi, V.; and Singh, P. (2020). Investigation of dimensional accuracy and international tolerance grades of 3D printed polycarbonate parts. *Materials Today: Proceedings*, 25, 537-543.
17. Abueidda, D.; Almasri, M.; Ammourah, R.; Ravaioli, U.; Jasiuk, I.; and Sobh, N. (2019). Prediction and optimization of mechanical properties of composites using convolutional neural networks. *Composite Structures*, 227, 111264.
18. Boschetto, A.; Giordano, V.; and Veniali, F. (2013). Surface roughness prediction in fused deposition modelling by neural networks. *The International Journal of Advanced Manufacturing Technology*, 67(9), 2727-2742.
19. Deswal, S.; Narang, R.; and Chhabra, D. (2019). Modeling and parametric optimization of FDM 3D printing process using hybrid techniques for enhancing dimensional preciseness. *International Journal on Interactive Design and Manufacturing*, 13, 1197–1214.
20. Barrios, J.M.; and Romero, P.E. (2019). Decision tree methods for predicting surface roughness in fused deposition modeling Parts. *Materials (Basel)*, 12(16), 1-10.
21. Padhi, S.; Sahu, R.K.; Mahapatra, S.; Das, H.; Sood, A.K.; Patro, D.B.; and Mondal, A. (2017). Optimization of fused deposition modeling process parameters using a fuzzy inference system coupled with Taguchi philosophy. *Advances in Manufacturing*, 5(3), 231-242.